# CROSS-BOUYANCY MIXED CONVECTION FROM A CONFINED SEMI-CIRCULAR CYLINDER IN A CHANNEL

**A DISSERTATION**

*Submitted in partial fulfilment of the*

*requirements for the award of the degree*

*of*

MASTER OF TECHNOLOGY

*in*

CHEMICAL ENGINEERING

*(With specialization in Industrial Safety and Hazard Management)*

**By**

**Manu K. Sukesan**

*(Enrolment No.-12516005)*


**DEPARTMENT OF CHEMICAL ENGINEERING**

**INDIAN INSTITUTE OF TECHNOLOGY ROORKEE**

**ROORKEE--247 667, UTTARAKHAND (INDIA)**

**JUNE-2014**

## DECLARATION

I hereby declare that the work presented in this Master's Thesis entitled "**Cross-buoyancy mixed convection from a confined semi-circular cylinder in a channel"** submitted towards completion of dissertation work of M.Tech. Chemical engineering (ISHM) at Indian Institute of Technology, Roorkee is an authentic record of my original work carried out under guidance of Dr. Amit Kumar Dhiman (IIT Roorkee). I have not submitted the matter embodied in this report for the award of any other degree.

Place : Roorkee — Manu K. Sukesan

Date : 12/06/2014 — Enrl. No. 12516005

---

## CERTIFICATE

This is to certify that Mr. Manu K. Sukesan (Enrol. No.12516005) has completed the Master's Thesis entitled "**Cross-buoyancy mixed convection from a confined semi-circular cylinder in a channel"** under my supervision.

**Dr. Amit Kumar Dhiman**

Associate Professor

Dept. of Chemical Engineering

IIT Roorkee

**Acknowledgement**

I would like to express my sincere gratitude to my supervisor, Dr. A. K. Dhiman for his encouragement, guidance and support. I would also like to thank Dr. V. K. Agarwal (Head of the department) for providing me with the opportunity and the resource for my dissertation work. I would like to acknowledge the selfless support of my parents for having utmost faith in me in whatever I did. Finally I would like to thank all the teaching and non-teaching staff of Chemical engineering Department for making my two years of M. Tech. a truly enriching educational experience.

Manu K. Sukesan

Enrl. No. 12516005

M. Tech. (I. S. H. M)

## CONTENTS


| Sr. No. | Title | Page No. |
|---|---|---|
| 1 | Declaration and Certificate | ii |
| 2 | Acknowledgement | iv |
| 3 | List of tables | v |
| 4 | List of figures | vi |
| 2 | Abstract | vii |
| 6 | List of publications | viii |
| 7 | Nomenclature | 1 |
| 8 | Chapter 1: Introduction | 2 |
| 9 | Chapter 2: Literature review | 5 |
| 10 | Chapter 3: Formulation and Numerical methodology | 10 |
| | 3.1 Grid dependence study | 13 |
| | 3.2 Domain dependence study | 15 |
| | 3.3 Time dependence | 17 |
| 11 | Chapter 4: Result and discussion | 18 |
| | 4.1 Validation of results | 18 |
| | 4.2 Flow and Thermal patterns | 20 |
| | 4.3 Variation of drag coefficient with Re, Ri and $\beta$ | 26 |
| | 4.4 Variation of lift coefficient with Re, Ri and $\beta$ | 28 |
| | 4.5 Local and Average Nusselt numbers | 29 |
| 12 | Chapter 5: Conclusion | 33 |
| 13 | Reference | 34 |

## LIST OF TABLES


| Sr. No. | Title | Page No. |
|---|---|---|
| 1A | Numerical results of a grid dependence study for a blockage ratio of 50% | 14 |
| 1B | Numerical results of a grid dependence study for a blockage ratio of 16.67% | 14 |
| 2 | Computational domains used for domain dependence study | 16 |
| 3 | Results of upstream dependence study for blockage ratios of 16.67% and 50% at Re=1 | 16 |
| 4 | Results of downstream dependence study for blockage ratios of 16.67% and 50% at Re=40 | 17 |
| 5A | Validation of present results of $C_D$ with ref. [11] at various values of Re | 19 |
| 5B | Validations of present results with refs. [14], [30] and [18]. | 19 |

## LIST OF FIGURES


| Sr. No | Title | Page No. |
|---|---|---|
| 1 | Schematic of the confined flow and heat transfer in a channel with a built-in semi-circular cylinder | 10 |
| 2 | Schematic representation of 2-D non-uniform computational grid structure for β=16.67% | 15 |
| 3A | Streamline contours at Re=1 and Pr=0.71 for different values of Richardson numbers and blockage ratios | 22 |
| 3B | Streamline contours at Re=40 and Pr=0.71 for different values of Richardson numbers and blockage ratios | 23 |
| 4A | Isotherm contours at Re=1 and Pr=0.71 for different values of Richardson numbers and blockage ratios | 24 |
| 4B | Isotherm contours at Re=40 and Pr=0.71 for different values of Richardson numbers and blockage ratios | 25 |
| 5 | Variation of friction drag coefficient, pressure drag coefficient and total drag coefficient with Reynolds and Richardson numbers and blockage ratio | 27 |
| 6 | Variation of the coefficient of lift with Reynolds number for different values of Ri and BR | 28 |
| 7 | Variation of local Nusselt number around curved and flat surfaces of a semi-circular cylinder for different values of Re, Ri and BR | 31 |
| 8. | Variation of average Nusselt number with Reynolds and Richardson numbers for different blockage ratios | 32 |

## ABSTRACT

The effects of cross-buoyancy on the flow and heat transfer characteristics of a long semi-circular bar in a confined channel have been investigated. The numerical results have been presented and discussed for the ranges of conditions as Reynolds number (Re) = 1 – 40, Richardson number (Ri) = 0– 4, and blockage ratio (β) =16.67% -50% for air as working fluid. The drag coefficient increases with increasing Richardson number and/or blockage ratio. The average Nusselt number is showing a maximum relative enhancement of approximately 8% for the Reynolds number of 40, Richardson number of 4 and for a wall confinement of 16.67%. On the other hand, the maximum relative variation of the coefficient of drag is found to be approximately 55% for the corresponding ranges of settings. Finally, the simple heat transfer correlations are obtained for the proceeding ranges of control parameters.



**Key words**: Semi-circular cylinder; Cross-buoyancy; Blockage ratio; Richardson number; Nusselt number; Drag and lift coefficients and Heat transfer enhancement.

## List of Publications

1. Manu K. Sukesan, Amit Dhiman, Cross-buoyancy mixed convection from a confined semi-circular cylinder, Int. comm. Heat Mass Transfer, revision submitted.

2. Manu K. Sukesan, Amit Dhiman, Laminar mixed convection from a semi-circular cylinder in an aiding buoyancy configuration: a validation study, International conference on advances in engineering and technology (ICAET-2014), Roorkee institute of Technology, Roorkee.

**NOMENCLATURE**

$\beta_V$ Coefficient of volumetric expansion,1/K

BR or $\beta$ Blockage ratio(=D/H)

$C_L$ Lift coefficient ($=F_L/(0.5\ U^2_\infty D)$)

$C_{DF}$ Friction drag coefficient

$C_{DP}$ Pressure drag coefficient

$C_D$ Total drag coefficient ($=F_D/(0.5\ U^2_\infty D)$)

$C_P$ Specific heat, J/(kg.K)

CV Control volume

D Diameter of a semi-circular cylinder, m

f Frequency ($s^{-1}$)

$F_D$ Drag force per unit length of the cylinder, N/m

$F_L$ Lift force per unit length of the cylinder, N/m

g Acceleration due to gravity, $m/s^2$

Gr Grashof number ( $= \frac{g\beta_V(T_W - T_\infty)\rho^2 D^3}{\mu^2}$ )

$\bar{h}$ Average heat transfer coefficient, $W/(m^2.K)$

$h$ Local heat transfer coefficient, $W/(m^2.K)$

H Domain height, m

k Thermal conductivity, W/(m.K)

L Length of computational domain ($=X_u+X_d$), m

n Power-law index

Nu Local Nusselt number( $= \frac{hD}{k}$ )

$\overline{Nu}$ Average Nusselt number ( $= \frac{\bar{h}D}{k}$ )

P Pressure (Pa)

Pr Prandtl number ( $= \frac{\mu C_P}{k}$ )

Re Reynolds number ( $= \frac{D\rho U_\infty}{\mu}$ )

Ri Richardson number ( $= Gr/\mathrm{Re}^2$ )

St Strouhal number ( $= fD/U_\infty$ )

t Time (s)

$T_\infty$ Free stream temperature, K

$T_w$ Cylinder surface temperature, K

T Temperature, K

$U_\infty$ Average velocity at inlet, m/s

$U_x$ Stream velocity in x direction, m/s

$U_y$ Stream velocity in y direction, m/s

$X_d$ Downstream distance, m

$X_u$ Upstream distance, m

$\alpha$ Thermal diffusivity

ρ Density of fluid, $kg/m^3$

μ Dynamic viscosity, $N.s/m^2$

γ Gap ratio

ν Kinematic viscosity, $m^2/s$

θ Dimensionless temperature ( $= \frac{T - T_\infty}{T_w - T_\infty}$ )

*Subscripts*

w Surface of the cylinder

∞ Inlet condition

*x* Stream wise coordinate, m

*y* Transverse coordinate, m

# Chapter-1: Introduction

Flow over a cylinder and alike structures is the area of interest for many decades for many researchers due to variety of its applications. Consequently, over the years, significant studies are now available in the literature on the flow around a semi-circular cylinder, but are mostly limited to unconfined domain. Flow over a semi-circular cylinder is encountered in tubular and pin type heat exchange systems, processing of fibrous suspensions, screens to dewater coal-water slurries, filtration of sewage sludge and polymer melts, removal of oversized particles from coating suspensions, polymer and food processing applications, flow metering devices, electronic cooling, probe and sensors, and others. Along the same line, mixed convection from a semi-circular cylinder in both the bounded and unbounded domains has received very less attention compared to flow over circular and square cylinders. In the present study, an attempt has been made to fill this gap for the confined flow around a heated semi-circular cylinder under the impact of cross-buoyancy mixed convection at low Reynolds numbers.

## 1.1 **Bluff body flow**

A boundary layer separation is always experienced by a bluff body when a fluid flows past it. Behind this bluff body (here the bluff body being semi-circular) very strong flow oscillations is observed in the wake region. A periodic flow motion will develop in the wake as a result of boundary layer vortex shedding from either side of cylinder at certain Reynolds number range. This regular pattern of vortices in the wake is called Karman Vortex Street which creates an oscillating flow at a discrete frequency.

## 2.2. **Newtonian fluids**

In continuum mechanics, a fluid is said to be Newtonian if the viscous stresses that arise from its flow, at every point, are proportional to the local strain rate. Most common fluids such as water, air gasoline and oils are Newtonian fluids.

$$\tau = \mu \frac{du}{dy}$$

Where $\tau$ and $du/dy$ is the shear stress and velocity gradient respectively. The constant of proportionality $\mu$ is known as the coefficient of viscosity

2.3. **Dimensionless groups**

The simple scaling and dimensional considerations of this flow suggest the following dimensionless number to characterize the flow.

2.3.1. **Reynolds number (Re)**

Reynolds number is a measure of the relative importance between the momentum flux by advection and by diffusion in the same direction.

$$\mathrm{Re} = \frac{D\rho U}{\mu}$$

Where, D, $\rho$, and U are the diameter of the cylinder, density of the fluid and average inlet velocity of the fluid respectively. $U_\infty$ is the free stream velocity for the confined flow.

2.3.2. **Prandtl number (Pr)**

It is a dimensionless number approximating the ratio of momentum diffusivity (kinematic viscosity) and thermal diffusivity.

$$\mathrm{Pr} = \frac{\mu C_P}{k}$$

Where, $C_p$ and $k$ are the specific heat and the thermal conductivity of the fluid, respectively.

For heat transfer problems, the Prandtl number controls the relative thickness of the momentum and thermal boundary layers..

2.3.3. **Nusselt number (Nu)**

In heat transfer at a boundary (surface) within a fluid, the Nusselt number is the ratio of convective to conductive heat transfer across (normal to) the boundary.

$$Nu = hD/k$$

Where, k= thermal conductivity of the fluid and h= convective heat transfer coefficient.

2.3.4. **Grashof number (Gr)**

The Grashof number is a dimensionless number in fluid dynamics and heat transfer which approximates the ratio of the buoyancy to viscous force acting on a fluid. It frequently arises in the study of situations involving natural convection.

$$\mathrm{Gr} = \frac{g\beta\Delta T\rho^2 D^3}{\mu^2}$$

Where g, β, $\Delta T$ are the coefficient of gravitational force, volumetric thermal expansion coefficient and temperature difference, respectively. At higher Grashof numbers, the boundary layer is turbulent; at lower Grashof numbers, the boundary layer is laminar.

### 2.3.5. **Richardson number (Ri)**

Richardson number is the dimensionless number and is equal to the ratio of potential to kinetic energy. Very less value (much less than unity) of Richardson number gives the unimportance of buoyancy in the flow and the value much greater than unity is considered as the buoyancy dominant flow

In thermal convection problems, Richardson number represents the importance of natural convection relative to the forced convection. The Richardson number in this context is defined as

$$Ri = Gr/\mathrm{Re}^2$$

Ri =0: Forced convection.

Ri= $\infty$ : Free convection.

Ri > 0: aiding flow mixed convection.

Ri < 0: Opposing flow mixed convection.

### 2.3.6 **Strouhal number (St)**

It is well known that the non-dimensional frequency of oscillation in lift is termed as Strouhal number.

$$\mathrm{St} = fL/U_\infty$$

Where f is the frequency of the vortex shedding and it is pertinent only in time-dependent flow regime. L is the characteristic length and $U_\infty$ is the velocity of the fluid. For large Strouhal numbers (order of 1), viscosity dominates fluid flow, resulting in a collective oscillating movement of the fluid "plug". For low Strouhal numbers (order of $10^{-4}$ and below), the high speed, quasi steady state portion of the movement dominates the oscillation. Oscillation at intermediate Strouhal number is characterized by the build-up and rapidly subsequent shedding of vortices.

# Chapter-2: Literature review

Kiya and Arie [1] studied the development of laminar boundary layer on semi-circular and semi-elliptical projections attached to a plane wall in the two-dimensional (2-D) viscous flow for the range of Reynolds numbers (Re) 0.1 to 100. They reported geometrical shapes of front and rear standing vortices, drag coefficients, pressure and shear-stress distributions as a function of Re. Experimentally, Boisaubert et al. [2] documented the influence of body shape upon the initial development of wake vortices by facing the round side and flat side of a semi-circular cylinder fitted with two end plate for the range of Reynolds numbers 60 to 600. They found the critical Reynolds number for the onset of vortex shedding as 140 and 190 for flat and curved surfaces, respectively. They also continued the study by the addition of a splitter plate (when, positioned along the downstream center plane) [3, 4] to find out the effect on near wake development. Coutanceau et al. [5] conducted an experiment to find out the way the initial wake vortices (primary and secondary) form and develop with time behind a short cylindrical semi-circular shell (hollow at the back). They reported that in lower-Re regime (Re = 60-100), the shedding takes place under a strong preliminary stretching of the vortices and then their splitting into two parts, whereas in the higher-Re regime (Re = 400-600), the vortices detach in one piece inducing a shortening of the formation zone. Kotake and Suwa [6] carried out an experiment by the use of visualization technique of the hydrogen bubble method in the uniform shear flow to find out the variation of stagnation points and the behaviour of vortices in the rear of semi-circular cylinder. They found out that, in the case of the shear flow, there was not a vortex on the side with the faster speed of the main stream and they also found that the vortex was generating only on the lower side. Iguchi and Terauchi [7] conducted an experimental study, by the usage of three kinds of non-circular (semi-circular, triangular and rectangular) cylinders to develop a Karman vortex probe capable of measuring a meniscus velocity lower than 10 cm/s and they reported that as long as the direction of flow approaching the triangular cylinder was known, then the triangular cylinder was found to meet this requirement most adequately. They also reported that for a minimum approaching velocity of 5 cm/s, an accurate measurement was possible. Sophy et al. [8] numerically investigated the flow past a semi-circular cylinder and they reported that for a circular cylinder, the Strouhal number

(St=0.166) obtained at Re=65 is 7% lesser than that of obtained in the case of semi-circular cylinder with the curved surface facing the flow. Koide et al. [9] made an investigation to find out the effect of movement of the separation point on circular, semi-circular and triangular cylinders by using a mechanical oscillator for cross-flow oscillation of the cylinders for a Reynolds number of about 3500. They reported that rather than an essential cause, the lock-in phenomenon is the reason for the movement of the separation point. They also reported that in spite of change in the span of the separation point movement, the lock-in region on the plane of non-dimensional cylinder frequency and amplitude was almost similar for all of the cylinders. Likewise, they [10] experimentally established the influence of cross-sectional configuration on Karman vortex excitation and they reported that the Karman vortex excitation appeared on the all three cylinders with remarkable different in oscillation behaviour.

To report the recent studies on the momentum and heat transfer characteristics, Chandra and Chhabra [11] carried out extensive numerical investigations for the span of Reynolds numbers (0.01 to 39.5) and Prandtl numbers ($Pr \leq 100$) on a semi-circular cylinder in an unconfined arrangement. The results elucidating that the first and second transition is seen in the range $0.55<Re<0.60$ and $39.5<Re<40$ respectively. Owing to the flat rear surface, both these transitions for circular and square cylinder occur at higher Reynolds numbers than that for semi-circular cylinder and this is due to the reduced streamlining and lack of symmetry about the y-axis of the bluff body. Gode et al. [12] have done the numerical investigation on a semi-circular cylinder for the range of value of Reynolds number ($0.01 \leq Re \leq 120$) and Prandtl number ($1 \leq Pr \leq 500$) for the maximum value of Peclet number being 4,000. The results show that as Reynolds number is increased, a smaller second wake is appeared at Re~33-34 likely to the large first wake at Re~20-22. Bhinder et al. [13] conducted a numerical study on a semi-circular cylinder for a large range of Reynolds numbers (80-180) by changing angles of incidences (0-$180^0$). They found that the streamline curvature is increased with increase in angle of incidence. They also observed the structural similarity between the vorticity contours and the corresponding isotherms. Chatterjee et al. [14] examined the 2-D unsteady fluid flow for the range of Reynolds number 50 to 150, for air as medium (Pr=0.71) over a semi-circular bluff body in an unconfined domain. The flow and thermal fields are reported to be more stable when the flow strikes on flat surface of a semi-circular cylinder rather that in the the curved surface. The coefficients of drag and lift for the flat surface arrangement are found to be more, but the frequency of vortex shedding and heat transfer rate are obtained more for the curved surface configuration. Chandra and Chhabra [15] also

numerically investigated the Newtonian /non-Newtonian flow over a semi-circular cylinder for the range of Re=0.01-40 and n=0.2-1.8 to find out the influence of power-law index (n) on the transition. Both the transition (as mentioned in ref. [13]) Reynolds numbers are found to be lowers than that for a circular cylinder and it is independent of type of fluid and its behaviour. Along the same line, they [16] simulated the flow and heat transfer for a range of Re= 0.01-30, Pr=1-100 and n=0.2-1.8 and they found that under suitable conditions, it is possible to enhance the heat transfer rate up to 60-70% in shear-thinning fluid. Lastly, simple expressions for wake length, surface pressure and Nusselt number have been derived.

On the mixed and natural convection across a semi-circular cylinder, Hocking and Vanden-Broeck [17] investigated the effect of gravity on the flow past a semi-circular cylinder with a constant pressure wake. The results indicate that the solutions are obtained as Froude number, cavitation number and arc length of the cavity change has effected significantly by the presence of gravity on the solutions. Also, they concluded that in the case of horizontal flow over a semi-cylinder, there are many solutions with stagnation point separation down to very small values of Froude number. Recently, Chandra and Chhabra examined the effect of mixed [18] and natural [19] convection around a semi-circular cylinder in the steady regime. The study about the effect of mixed convection [18] reports the flow and transfer of heat from a heated semi-circular cylinder immersed in power-law fluids with its curved surface facing upstream for Re=1-30, Ri=0-2, Pr=1-100 and n=0.2-1.8. The maximum value of Nu at corners are observed at low Reynolds numbers (such as Re = 1), and for high values of the Reynolds numbers it shifts toward the front stagnation point. They also reported that the average Nusselt number increases with Re, Pr and Ri. Similarly, Tiwari and Chhabra [20] numerically studied the laminar free convection heat transfer from a heated semi-circular cylinder, immersed in dormant power-law fluids with the flat face of the bluff body facing downward, for the following span of parameters: $10 \leq Gr \leq 10^5$, $0.72 \leq Pr \leq 100$, and $0.2 \leq n \leq 1.8$. They observed that, irrespective of the value of n, both Nu and $\overline{Nu}$ show a positive dependence on Gr and Pr. Chandra and Chhabra [21] also studied the vortex shedding regime for the forced and heat transfer flow throughout a semi-circular cylinder for the span of conditions as Re=40-140, Pr=0.7-50 and n=0.2-1.8. By the increment of Pr from 0.7 to 50, the average Nusselt number increases by a factor of 5-6, which is in line with the expected scaling of $\overline{Nu} \sim Pr^{1/3}$. As far as we know, only Can and Celik [22] did a numerical investigation on a semi-cylindrical obstacle situated between two adiabatic walls to observe the effect of flow and transfer of heat for the high range of

Reynolds numbers $10^4$ to $10^5$ for the fixed values of Prandtl number (0.71) and blockage ratio (25%). With increase in turbulence level on the upper side of the semi-circular cylinder, there is an increment in local Nu value is observed. They also reported that the curved part of a semi-circular cylinder which facing the flow showed small variations when compared to flat portion of a semi-circular cylinder which facing the flow.

Because no literature is available on the flow and heat transfer phenomena over a semi-circular cylinder in the confined domain at low Reynolds numbers and to make the literature review section more comprehensive, the pertaining studies on the other frequently encountered bluff bodies such as circular and square confined in a channel are discussed next. Singh et al. [23] made a numerical investigation on the mixed convection from a circular cylinder which is heated/cooled in a vertical channel for the fixed values of Reynolds number (100), Prandtl number (0.71), and blockage ratio (25%) for the range of Ri values ($-1 \leq Ri \leq +1$). They reported that at a Ri value of about 0.15, breakdown of Karman Vortex Street were occurred. Gandikota et al. [24] investigated the result of aiding/opposing buoyancy throughout the 2-D circular cylinder which is confined for the blockage ratios of 2% and 25% at Re = 50–150 and Ri = -0.5 to +0.5. They observed that the critical Ri (i.e., the onset of vortex shedding) is rising with Re and it is also observed that decreasing blockage ratio increases the critical Ri at any Re. In the negative Ri ranges, $\overline{Nu}$ remains almost constant but it increases at a faster rate beyond the critical Ri. On the other hand, Dhiman et al. [25] simulated the effect of cross-buoyancy mixed convection and of Prandtl number on the flow and heat transfer characteristics of an isothermal square cylinder confined in a channel for the fixed blockage ratio of 12.5% at Re=1-30, Ri=0-1 and Pr=0.7-100. They reported that an increment up to 5% is observed in the value of the average Nusselt number about the pure forced convection value (Ri=0) and the influence of the Ri on the $C_D$ and $\overline{Nu}$ is qualitatively similar to the case of the unconfined mixed convection. Subsequently, Dhiman et al. [26] numerically investigated the effects of blockage ratios on the confined mixed convection from a long heated square obstacle confined in a horizontal channel. The numerical computations are performed in the steady regime for Re=1-30, Ri =0-1 for $\beta$=12.5%-25% for the fixed Prandtl number of 0.7. They reported that with increase in value of the blockage ratio, asymmetry in the flow and temperature fields decreases. They also reported that for the fixed values of Reynolds and Richardson numbers, the $C_D$ value increases with increase in the value of the blockage ratio. Recently, Dhiman et al. [27] examined the confined upward flow and heat transfer around a square cylinder under the effect of aiding buoyancy (Ri=0–1) in the vertical channel for Re=1–40 and $\beta$=25–50% for air as

working fluid. They found that the $C_D$ increases with both aiding buoyancy and wall confinement but it decreases with the Re. At the same time the $\overline{Nu}$ increases with both Re and Ri. Similarly, Sharma et al. [28] studied the momentum and heat transfer characteristics of the laminar flow of power-law fluids in a vertical channel with a built-in square cylinder under aiding buoyancy for the range of settings as Re=1-40, Ri=0-1, n=0.4-1, $\beta$=25%-50% and Pr=50. It is found that the $C_D$ and $\overline{Nu}$ increases with the aiding buoyancy, while the shear-thinning behaviour reduces the $C_D$ and increases the rate of heat transfer.

Thus, from the above discussion, one can conclude that sufficient information is now available in the literature on the forced convection flow and heat transfer (Ri=0) around a long semi-circular bar in the unconfined domain. On the contrary, only Chandra and Chhabra [18] systematically investigated the aiding buoyancy mixed convection around a semi-circular bluff body in the unconfined domain. Unfortunately, the knowledge about the mixed convection on a semi-circular cylinder in a confined channel as far as we know is unavailable in the literature. So the main focus of this study is to find out the effects of Reynolds and Richardson numbers and blockage ratio on the mixed convection from a heated semi-circular cylinder in a confined channel under cross-buoyancy at low Reynolds numbers.

# Chapter 3: Formulation and numerical methodology

In the present study, the 2-D numerical computations were carried out for a long semi-circular cylinder fitted in a confined horizontal channel at an upstream distance of $X_u/D$ from inlet and at a downstream distance of $X_d/D$ from outlet (Fig. 1). The semi-circular body is exposed to a laminar fully developed flow of incompressible fluid having uniform temperature ($T_\infty$) of 298K with an average velocity $U_\infty$.

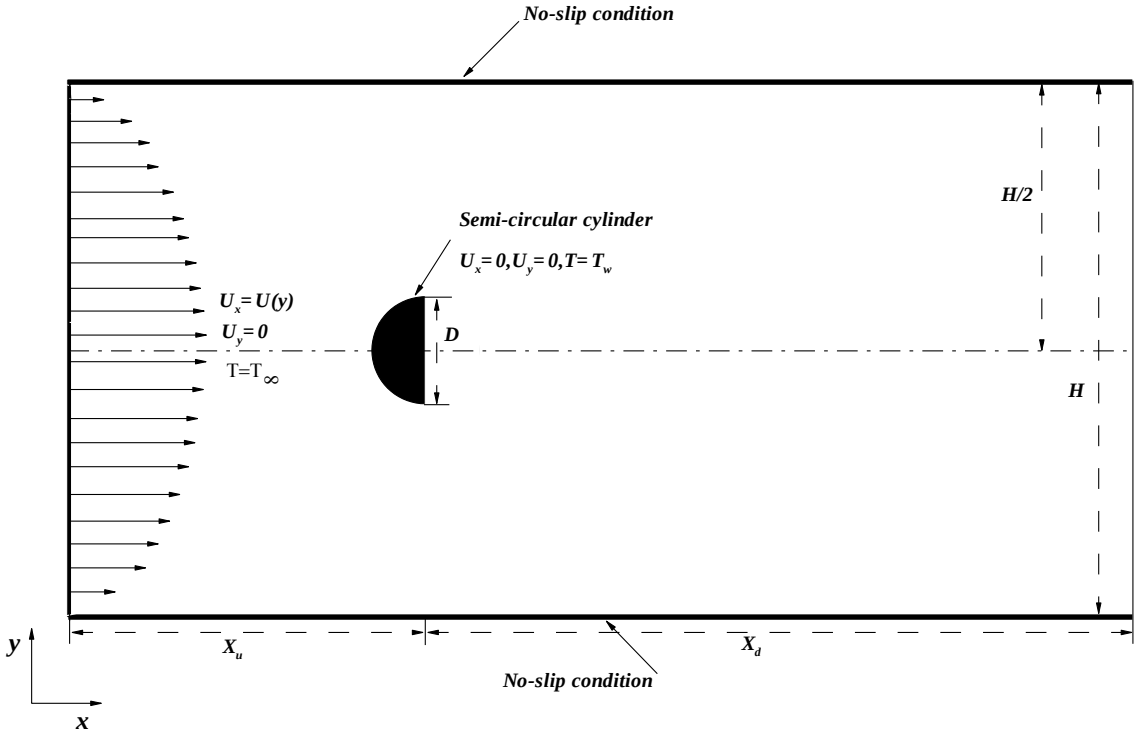


Fig 1: Schematic of the confined flow and heat transfer in a channel with a built-in semi-circular cylinder

We have considered air as the working fluid with constant Prandtl number of 0.71. The obstacle is located on the centreline of the channel and it is maintained at a temperature ( $T_w$ ) of 300K. The channel wall confinement or blockage ratio (β) is defined here as $D/H$ , where *D* is the diameter of the semi-circular cylinder and *H* is the distance between confined walls.

The continuity, *x*- and *y*- components of Navier-Stokes and thermal energy equations are given as follows

Continuity equation

$$\frac{\partial U_x}{\partial x}+\frac{\partial U_y}{\partial y}=0 \tag{1}$$

Momentum equations

$$\frac{\partial U_x}{\partial t}+\frac{\partial U_x U_x}{\partial x}+\frac{\partial U_y U_x}{\partial y}=-\frac{1}{\rho}\frac{\partial P}{\partial x}+\nu\left(\frac{\partial^2 U_x}{\partial x^2}+\frac{\partial^2 U_x}{\partial y^2}\right) \tag{2a}$$

$$\frac{\partial U_y}{\partial t}+\frac{\partial U_x U_y}{\partial y}+\frac{\partial U_y U_y}{\partial y}=-\frac{1}{\rho}\frac{\partial P}{\partial y}+\nu\left(\frac{\partial^2 U_y}{\partial x^2}+\frac{\partial^2 U_y}{\partial y^2}\right)+RiT \tag{2b}$$

Energy equation

$$\frac{\partial T}{\partial t}+\frac{\partial U_x T}{\partial x}+\frac{\partial U_y T}{\partial y}=\alpha\left(\frac{\partial^2 T}{\partial x^2}+\frac{\partial^2 T}{\partial y^2}\right) \tag{3}$$

Where $U_x$, $U_y$, *P*, *T* are the *x* and *y* components of velocity, pressure and temperature respectively. *v* is the kinematic viscosity ( $\frac{\mu}{\rho}$ ) and $\alpha$ is the thermal diffusivity ( $\frac{k}{(\rho C_P)}$ ). Here, flow and heat transfer phenomena are governed by three dimensionless groups namely Re, Ri and Pr, which are defined as Reynolds number $(\mathrm{Re})=\frac{\rho U_\infty D}{\mu}$ , Richardson number $(Ri)=\frac{Gr}{\mathrm{Re}^2}$ and Prandtl number $(\mathrm{Pr})=\frac{\mu C_P}{k}$ respectively.

The following boundary conditions may be written for the present system.

*The fully developed velocity profile for the laminar flow in a channel with height H is given by*

$$U_x = 1.5U_\infty[1-(\left|1-\frac{2y}{H}\right|)^2] \ (0 \le y \le H)$$

- *At the channel inlet* ($x$=0): $U_x = U(y)$, $U_y = 0$ *and* $T = T_\infty$
- *On upper and lower walls of the channel:* $U_x = 0$, $U_y = 0$ (no-slip) and $\partial T / \partial y = 0$ (adiabatic)
- *At the surface of a semi-circular cylinder:* $U_x = 0, U_y = 0$ (no-slip) and $T = T_w$ (uniform wall temperature condition)
- *At the channel exit* ($x$=$L$): $\partial U_x / \partial x = 0$ , $\partial U_y / \partial x = 0$ and $\partial T / \partial x = 0$

A commercial finite volume method based solver Ansys Fluent [29] is being used to solve governing equations along with above mentioned boundary conditions. The 2-D steady/ unsteady, laminar, segregated solver is used to solve the incompressible flow on the collocated grid system. To discretize convective terms of momentum and energy equations, the Quick scheme is being utilized. Also, to incorporate the fully developed velocity profile at the channel inlet, the user defined functions available in Ansys [29] are exploited. The Semi-Implicit Method for the Pressure Linked Equations algorithm is used to circumvent pressure-velocity decoupling. The algebraic equations resulting after linearization are solved by using the Gauss-Seidel iterative method in conjunction with an Algebraic Multi Grid solver (AMG). The use of AMG method considerably decrease the number of iterations and thus the central processing unit time needed to acquire a converged solution. The relative convergence criteria of $10^{-10}$ each and $10^{-20}$ each are used for the residuals of continuity, $x$-momentum, $y$-momentum and energy equations in steady and unsteady regimes, respectively.

## GRID, DOMAIN AND TIME DEPENDENCE STUDIES

### 3.1 GRID DEPENDENCE

It is apparent that the accuracy of the result will increase with increase in number of control volumes (CVs), but it will result in increased computational time and power, so there should be a compromise between number of control volumes and computational time. This can be done by the usage of a good and economical grid for simulation. To conduct a grid dependence study, three grids were generated and studied for Re=40, Ri=0, Pr=0.71 and for the extreme blockage ratios of 50% and 16.67%.

The grid structures details are given in Tables 1A and 1B along with the corresponding output parameters like $C_D$ and $\overline{Nu}$. The grid structures symbolically represented as G1, G2 and G3 are showing the maximum deviation of about 2.15% for a blockage ratio of 50% and the percentage relative difference between G1 & G2 for the values of $C_D$ and $\overline{Nu}$ are about 2.15% and about 0.84% respectively. At the same time, the values of $C_D$ and $\overline{Nu}$ for the grid G2 are showing only a variation of about 0.02% and about 0.45% respectively with respect to G3 (Table 1A). At blockage ratios of 16.67% and 50% for three different grid structures (G1, G2 and G3), the grid structure G2 is selected as an optimum one for further studies because it is giving considerable accuracy with less computational time and is shown in Fig. 2. Figure 2 shows the enlarged view of the optimized grid (G2) around a semi-circular cylinder. In order to capture the steep gradients near the surface of the semi-circular cylinder, sufficiently fine grid was preferred in the vicinity of the cylinder. The details of the total number of cells in the domain and the CVs around the cylinder can be seen in Tables 1A and 1B for $\beta$ =50% and 16.67% respectively.

Table 1A: Numerical results of a grid dependence study for a blockage ratio of 50%

| Grid | CVs on cylinder surface | Total number of cells | $C_D$ | $\overline{Nu}$ |
|---|---|---|---|---|
| G1 | 250 | 43436 | 9.521 | 4.394 |
| G2 | 340 | 103579 | 9.321 | 4.431 |
| G3 | 400 | 127691 | 9.319 | 4.451 |

Table 1B: Numerical results of a grid dependence study for a blockage ratio of 16.67%

| Grid | CVs on cylinder surface | Total number of cells | $C_D$ | $\overline{Nu}$ |
|---|---|---|---|---|
| G1 | 250 | 68484 | 3.381 | 3.635 |
| G2 | 340 | 115585 | 3.336 | 3.665 |
| G3 | 400 | 140691 | 3.330 | 3.684 |

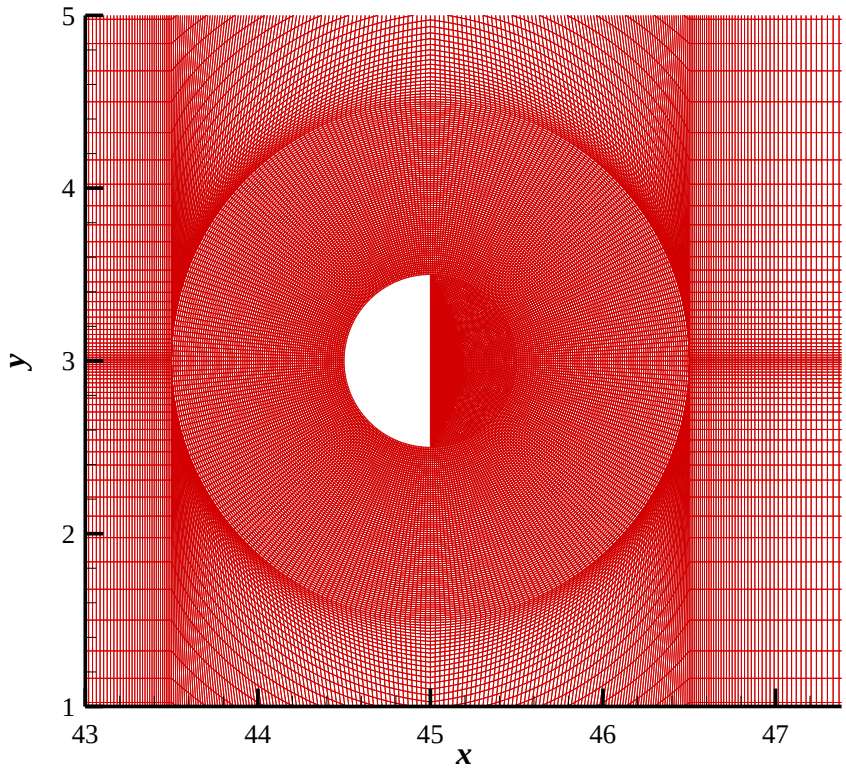


Fig.2: Schematic representation of 2-D non-uniform computational grid structure for β=16.67% (magnified view around a semi-circular cylinder)

## 3.2 DOMAIN DEPENDENCE

In the domain dependence study, three types of domains were generated (given in Table 2) and tested for the extreme value of Richardson number of 4 and the results obtained are illustrated in Tables 3 and 4. Two extremes values of Reynolds numbers (1 and 40) and blockage ratios (16.67% and 50%) are used to find out the optimum computational domain for further studies by assuming that the effects of physical parameters within this range will be minimum. For low Reynolds number (e.g. Re=1), upstream effect is more predominant and for high Re value (e.g. Re=40) downstream effect is more predominant. Therefore, the upstream dependence study is conducted at Re=1 by keeping downstream distance constant (i.e. 120D) and by simply varying the upstream distance from 45D to 60D (i.e. Domains I and III). The results are showing no variations for the blockage ratio of 50% as the values obtained were the same. But it's showing a variation of only about 0.01% on drag coefficient for the blockage ratio of 16.67% (Table 3). Similarly, the downstream distance is varied from 120D to 140D

(Domains I and II) by keeping upstream distance constant as 45D at Re=40. Again, the results are found same at $\beta$=50%. However, the maximum variation is found to be about 3.5% for the lift coefficient for a blockage ratio of 16.67%, and of the drag coefficient and $\overline{Nu}$ is showing the variations of about 2.9% and about 1.4% respectively. So the Domain I (i.e. $X_u$=45D and $X_d$=120D) is used for further studies because number of control volumes on Domain I is less compared to other domains, and it results in less computational time and power.

Table 2: Computational domains used for domain dependence study

| Domain | Upstream distance | Downstream distance | Control volumes |
|---|---|---|---|
| I | 45D | 120D | 103579 |
| II | 45D | 140D | 107579 |
| III | 60D | 120D | 106579 |

Table 3: Results of upstream dependence study for blockage ratios of 16.67% and 50% at Re=1

| BR and Domain | $C_D$ | $C_L$ | $\overline{Nu}$ |
|---|---|---|---|
| BR=50%,Domain-III | 211.3889 | -1.2783 | 0.4322 |
| BR=50%,Domain-I | 211.3889 | -1.2783 | 0.4322 |
| BR=16.67%,Domain-III | 95.7259 | 2.2757 | 0.9541 |
| BR=16.67%,Domain-I | 95.7360 | 2.2757 | 0.9541 |

Table 4: Results of downstream dependence study for blockage ratios of 16.67% and 50% at Re=40

| BR and domain | $C_D$ | $C_L$ | $\overline{Nu}$ |
|---|---|---|---|
| BR=50%,Domain-II | 9.5727 | -1.5617 | 4.4718 |
| BR=50%,Domain-I | 9.5727 | -1.5617 | 4.4718 |
| BR=16.67%,Domain-II | 10.5620 | -0.7278 | 5.0688 |
| BR=16.67%,Domain-I | 10.2650 | -0.7030 | 4.9950 |

## 3.3 TIME DEPENDENCE

To converge the solution more speedily and reliably require a choice of an optimum time step and at the same time it must not compromise with the accuracy of result. In this study, two time steps were considered as 0.008D and 0.01D. As expected, the time step of 0.008D will provide more accurate solution, but resulting in higher computational time compared to the time step of 0.01D. For this, numerical simulations were carried out for the highest Reynolds number of 40, Richardson number of 4 for the two extreme values of blockage ratios of 16.67% and 50%. For a blockage ratio of 50%, there is negligible difference in the output parameters, and for the blockage ratio of 16.67% the maximum variation is found to be below 0.1%. So the use of dimensionless time step of 0.01 is found adequate with considerable accuracy and computational time for the further numerical investigations.

# Chapter 4: Result and Discussion

The section provides the systematic details on the flow and heat transfer phenomena for laminar incompressible Newtonian flow over a semi-circular cylinder situated in a confined channel under cross-buoyancy for the controlling parameters like Re, Ri and $\beta$ ranging from 1-40, 0-4 and 16.67%-50% respectively for air as working fluid.

## 4.1 VALIDATION

The present study used four standard studies to establish the validity of the present numerical simulation approach. First validation is done with Chandra and Chhabra's [11] observations and the present results are showing an excellent agreement with ref. [11]. For instance, the maximum deviation of only about 0.06% with ref. [11] is observed and the comparison is shown in Table 5A at various values of Re. Secondly, the results are simulated for an unconfined flow over a semi-circular cylinder and are benchmarked with the results of Chatterjee et al. [14] in Table 5B. The present values are showing a good agreement with ref. [14] and a deviation is within 1.3% for the coefficient of drag and about 4% for the average Nusselt number at Re=150 and Pr=0.71. The reason for some variation in the results of two studies is because of the difference in total number of cells utilized in the computational domain. The values of drag coefficient ($C_D$), Strouhal number (St) and Nusselt number ( $\overline{Nu}$ ) along with total number of cells in the domain are given in Table 5B. The third validation is done with the results of Srinivas et al. [30] for a circular cylinder under the impact of aiding buoyancy. For this, the mixed convection from an unconfined heated circular cylinder immersed in an incompressible Newtonian fluid is studied and the comparison of $C_D$ and $\overline{Nu}$ results is reported in Table 5B. Like previous validations, the present results are in an excellent agreement with ref. [30] and the total drag coefficient is showing variations of about 0.12% and 0.36% for Reynolds numbers of 1 and 40 respectively. However, the average Nusselt number is showing variations of only about 0.006% and 0.08% for Re values 1 and 40 respectively. The last validation is done with Chandra and Chhabra's[18] observation of mixed convection on semi-circular cylinder under the impact of aiding buoyancy and the values are shown in Tables 5B . The maximum variation for the average Nusselt number and $C_D$ is found to be 2.5% and 0.37% respectively for Reynolds number 30 and Richardson number 2. This validates the present solution methodology.

Table 5A: Validation of present result of CD with ref.[11] at various values of Re

| Re | Present work | Chandra and Chhabra[11] |
|---|---|---|
| 1 | 10.050 | 10.055 |
| 5 | 3.832 | 3.832 |
| 10 | 2.709 | 2.710 |
| 20 | 1.993 | 1.993 |
| 30 | 1.690 | 1.691 |

Table 5B: Validations of present results with refs. [14], [30] and [18].

| Validation of present results with ref. [14] at Pr=0.71 (Total No. of cells for present work=147439, Total No. of cells for ref.[14]= 119000) | | | |
|---|---|---|---|
| Re | Output parameters | Present work | Values from literature |
| 150 | $C_D$ | 1.7354 | 1.7580 |
| | St | 0.1978 | 0.1981 |
| | $\overline{Nu}$ | 7.4004 | 7.6969 |
| Validation of present results with ref. [30] for Re=1 and 40 at Pr=50 | | | |
| 1 | $C_D$ | 15.2150 | 15.1969 |
| | $\overline{Nu}$ | 2.9978 | 2.9976 |
| 40 | $C_D$ | 2.1250 | 2.1173 |
| | $\overline{Nu}$ | 15.1479 | 15.1594 |
| Validation of present results with ref. [18] at Pr=1 for different Re and Ri | | | |
| Ri=0 | | | |
| 1 | $C_D$ | 10.1402 | 10.170 |
| | $\overline{Nu}$ | 0.9680 | 0.979 |
| 10 | $C_D$ | 2.7169 | 2.721 |
| | $\overline{Nu}$ | 2.1617 | 2.205 |
| 30 | $C_D$ | 1.6937 | 1.696 |
| | $\overline{Nu}$ | 3.3783 | 3.460 |
| Ri=2 | | | |
| 1 | $C_D$ | 34.9790 | 35.10 |
| | $\overline{Nu}$ | 1.2431 | 1.260 |
| 10 | $C_D$ | 7.9235 | 7.945 |
| | $\overline{Nu}$ | 2.7208 | 2.778 |
| 30 | $C_D$ | 4.8711 | 4.889 |
| | $\overline{Nu}$ | 4.1984 | 4.306 |

## 4.2. FLOW AND THERMAL PATTERNS

The detailed flow patterns in the vicinity of a long semi-circular cylinder are presented in Figs. 3A (a-i) and 3B (a-i) by streamline contours for the two extreme values of Reynolds numbers 1 and 40 respectively and for the range of Richardson number=0 (forced convection) to 4 at various blockage ratios (50% to 16.67%). The flow is found to be symmetric about the centre line for forced convection (Ri=0) for the range of Reynolds numbers studied. The flow is found asymmetric for the Reynolds number of unity for mixed convection (Ri=1 and 4). This is because of the effect of superimposed thermal buoyancy on the flow. No flow separation is found at Re=1 for Ri=0-4 for the blockage ratios of 16.67%, 25% and 50%. However, the flow separation is found to be occurred above Reynolds number of unity. The flow pattern appears to be similar to ref. [18] for the semi-circular cylinder and to the flow over a square cylinder situated in a confined channel [25, 26]. The degree of asymmetry is increased with increase in the value of Richardson number for different values of blockage ratios as shown in Figs. 3A (a-i).

For instance, higher blockage ratio (e.g. 50%) is showing more flow symmetry as compared to lower blockage ratio (e.g. 16.67%). This is due to the fact that the flow tends to stabilize with increase in the value of the blockage ratio as well as the cross-buoyancy effects decrease. These findings are also consistent with ref. [26] for the confined flow around a square cylinder under cross-buoyancy mixed convection. Furthermore, a wake region is also observed above the semi-circular cylinder for the high value of Reynolds number of 40 and the low value of blockage ratio of 16.67% at Ri=4 (Fig. 3Bi). Similar flow structure is also obtained for the flow over a square cylinder for the Reynolds numbers below 40 [26]. This is due to the flow reversal at the top channel wall due to higher mass flow rate below the semi-circular cylinder than above it. The flow is found to be time-periodic for Re=40 and Ri=1 for the low value of blockage ratio of 16.67% (Fig. 3Bf), because of the occurrence of von Karman vortex shedding.

The temperature field around the semi-circular cylinder is represented by isotherm patterns for the extreme values of Reynolds numbers, Richardson numbers and blockage ratios for a constant Prandtl number of 0.71 (air) and is shown in Figs. 4A(a-i) and 4B(a-i). More crowding of temperature contours is observed near to the curved surface of a semi-circular cylinder compared to the flat surface, which results in a higher value of Nusselt number on the curved surface of a semi-circular cylinder. The crowding of temperature contours is found to be increased with increase in Reynolds number and

this result indicating that the heat transfer is increasing with increase in Reynolds number. The lateral thinning of temperature contours are also observed at high Reynolds numbers (e.g. Re=40). Similar to flow pattern, an increase in asymmetry of isotherms is observed with increase in Richardson number .This can be explained as at higher Richardson number, the effect of superimposed thermal buoyancy is high. This effect is more predominant in low blockage ratios (e.g. 16.67%). The similar observations are also reported for the confined square cylinder under cross-buoyancy [26]. Because of the occurrence of von Karman vortex shedding in the flow field, the thermal pattern is found to be time-periodic at Re=40, Ri=1 and $\beta$ =16.67%.

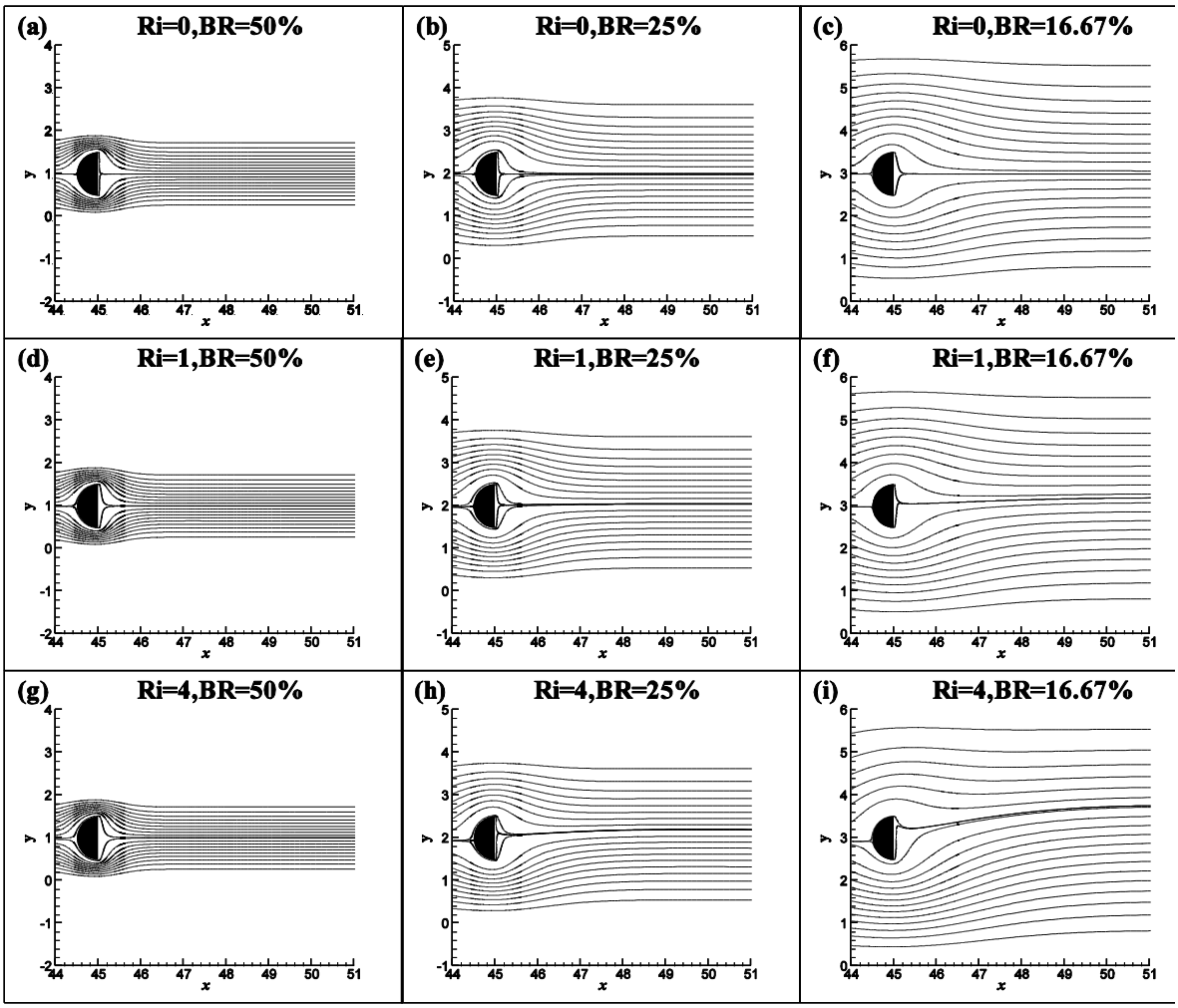


Fig. 3A: Streamline contours at Re=1 and Pr=0.71 for different values of Richardson numbers and blockage ratios

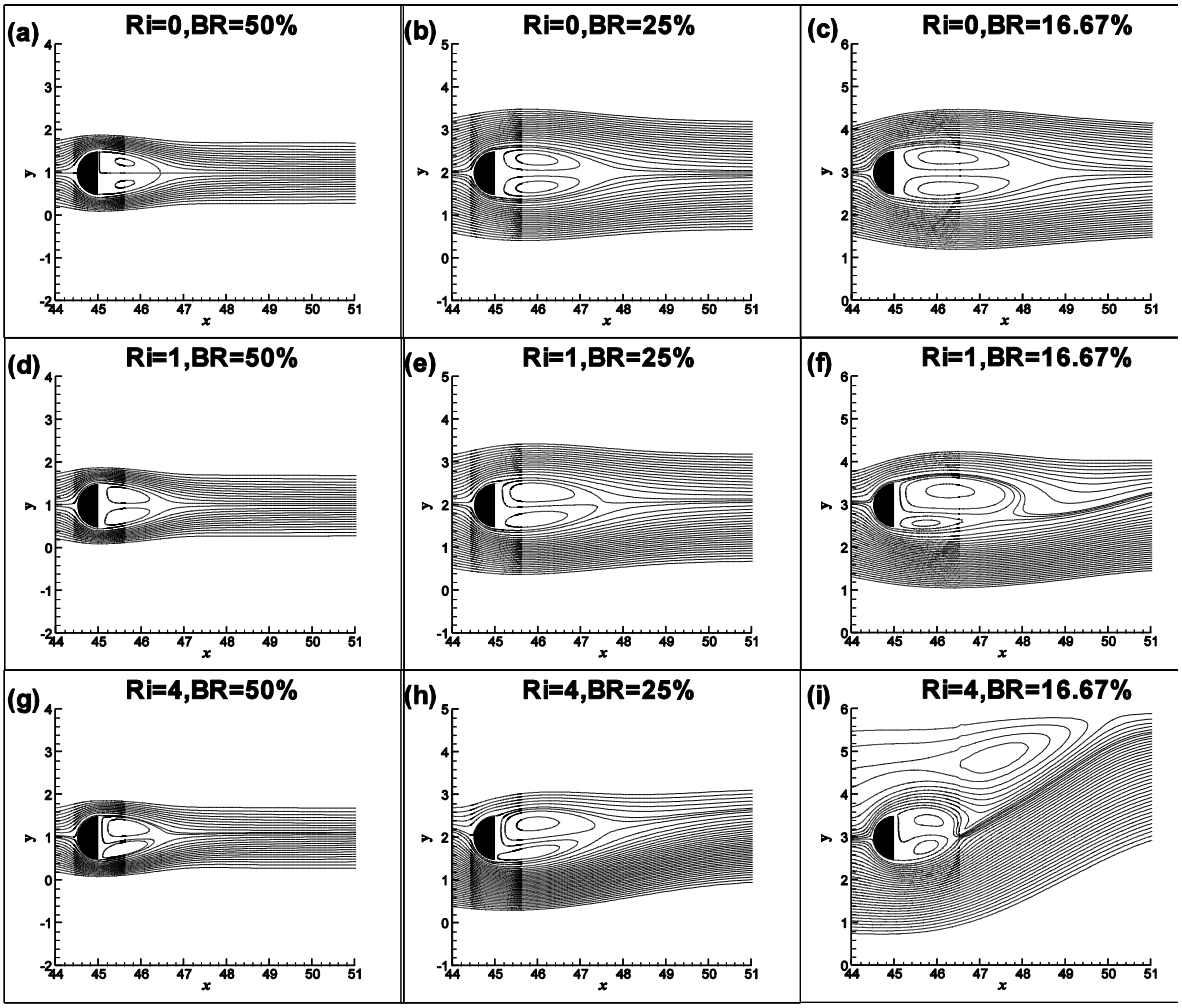


Fig. 3B: Streamline contours at Re=40 and Pr=0.71 for different values of Richardson numbers and blockage ratios

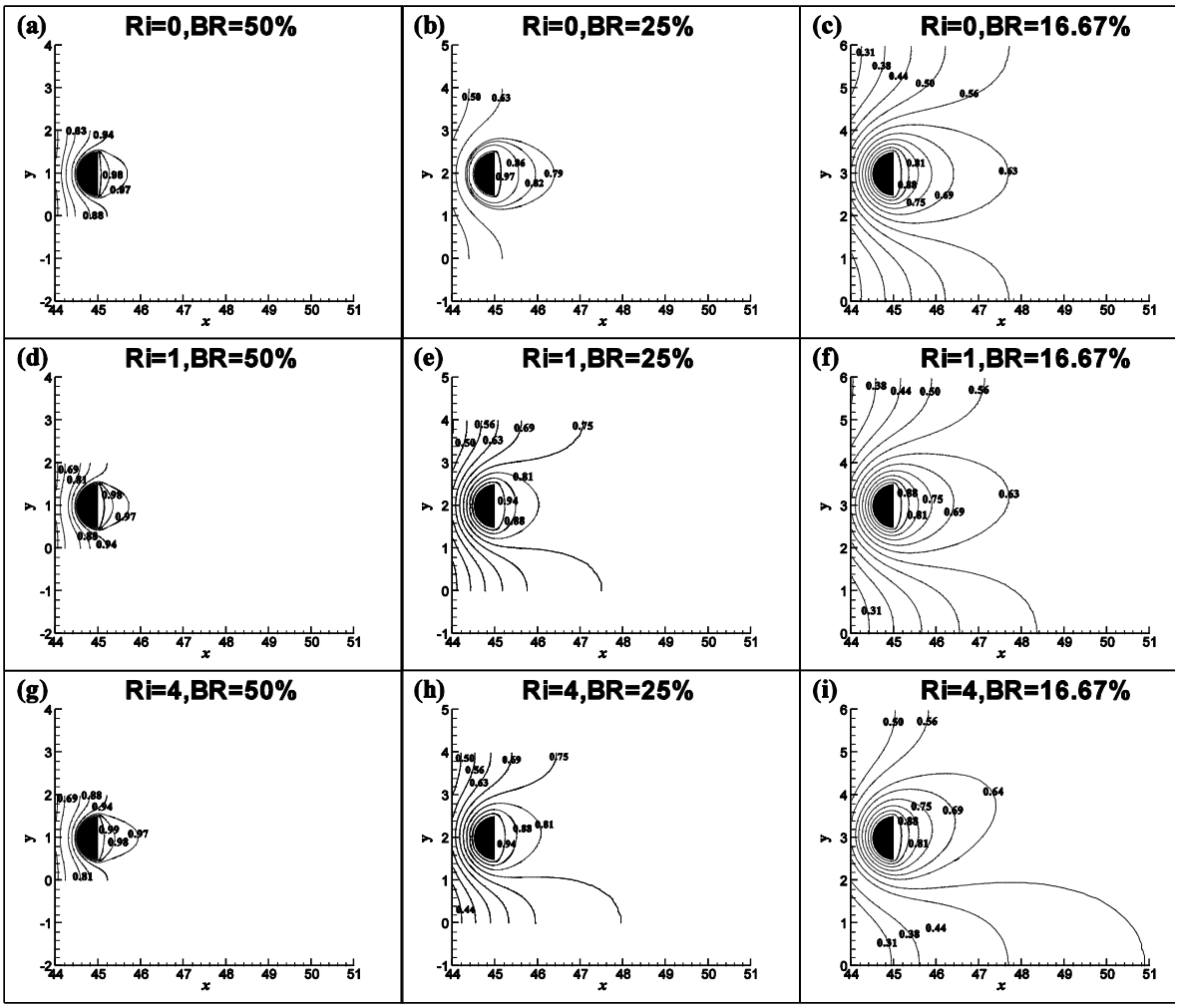


Fig. 4A: Isotherm contours at Re=1 and Pr=0.71 for different values of Richardson numbers and blockage ratios. The dimensionless values of temperature contours (θ) are also indicated herein

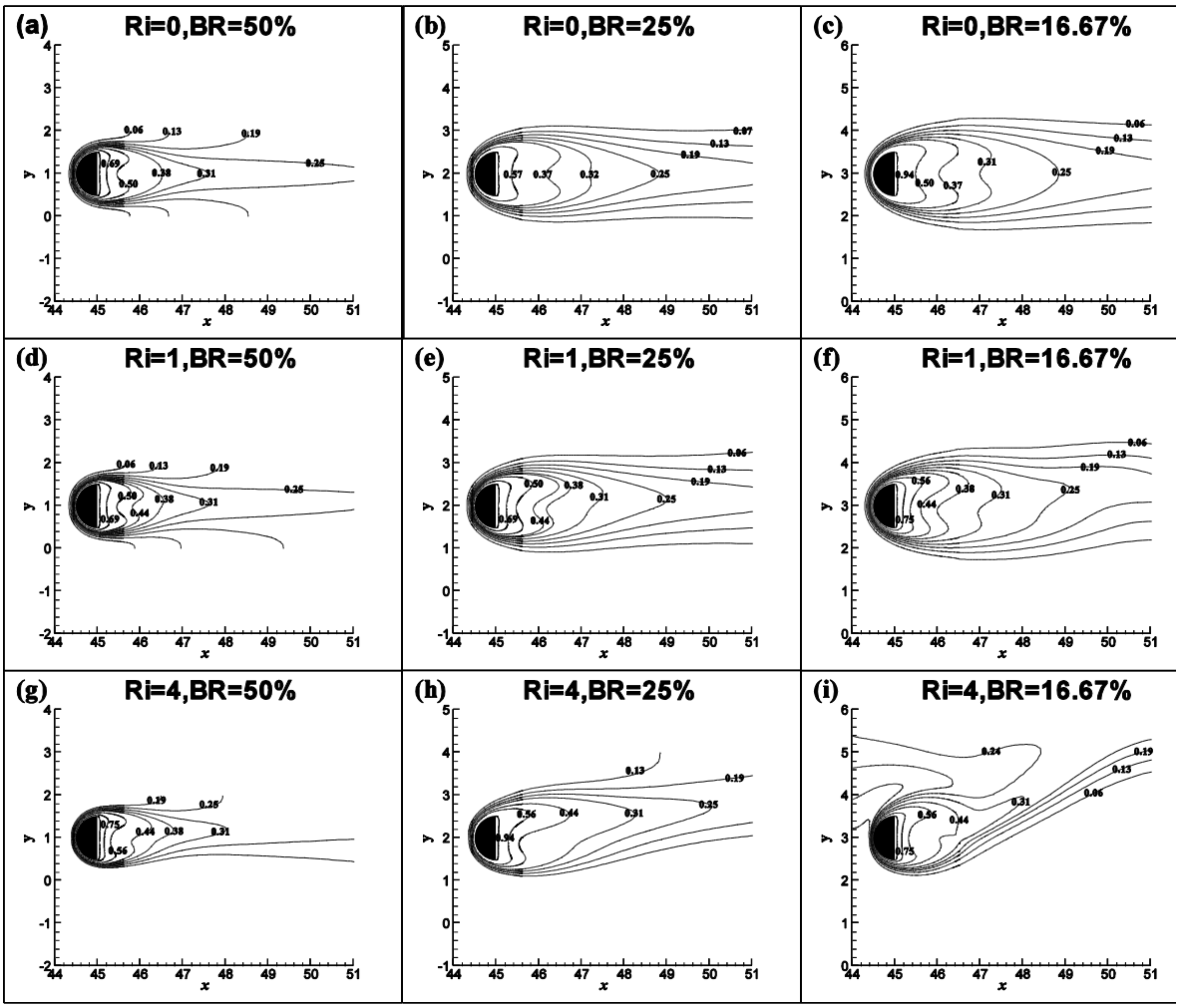


Fig. 4B: Isotherm contours at Re=40 and Pr=0.71 for different values of Richardson numbers and blockage ratios. The dimensionless values of temperature contours (θ) are also indicated herein

### 4.3. VARIATION OF DRAG COEFFICIENTS WITH Re, Ri AND $\boldsymbol{\beta}$

The overall drag coefficient and its components for different Reynolds number, Richardson number and blockage ratio are calculated and plotted in Fig. 5 in the steady regime. The overall drag coefficient is showing the decreasing behaviour with increase in the value of Reynolds number for the constant values of blockage ratio and Richardson number. These observations are similar to the observations of flow over unconfined semi-circular cylinder [18]. It is found out that the pressure drag coefficient is contributing major part for the total drag coefficient. The friction drag coefficient and the pressure drag coefficient are also decreasing with increase in the value of Reynolds number (Figs. 5a-5f). The graph also shows that as we move from low blockage ratio (16.67%) to high (50%) for the constant Reynolds number and Richardson number, the drag coefficient increases. This is because of the facts that with the increasing blockage, the regions for the flow between the boundary layers of heated and unheated walls decrease due to more confinement. It is also worthwhile to mention that the flow is found to be time-periodic for Re=40 and Ri=1 for the low blockage ratio of 16.67% and the Strouhal number for this flow is found to be 0.18. It is find to be insignificant to find out the $C_{DF}$ and $C_{DP}$ values at Re=40, Ri=1 and BR=16.67%. So the graph is truncated up to Re=20 for the BR=16.67%.

The drag coefficient also increases with increase in the value of Richardson number for the constant values of Reynolds number (similar to ref. [18]) and blockage ratio, and shows a maximum enhancement of approximately 55% for Reynolds number of 40, Richardson number of 4 and blockage ratio of 16.67%. Because the variations in drag coefficient increase with decrease in the value of blockage ratio, the maximum variations are observed for the low blockage ratio of 16.67%. This is because of the decreasing buoyancy effects with increasing $\beta$ as also reported for the confined square cylinder in refs. [25, 26]. It is also worthwhile to mention that the total drag coefficient is found to be higher for confined semi-circular cylinder compared to unconfined semi-circular cylinder [18]. Furthermore, the present total drag coefficient is found to be less compared to the flow over a square cylinder situated in a confined space with the aid of buoyancy [27].

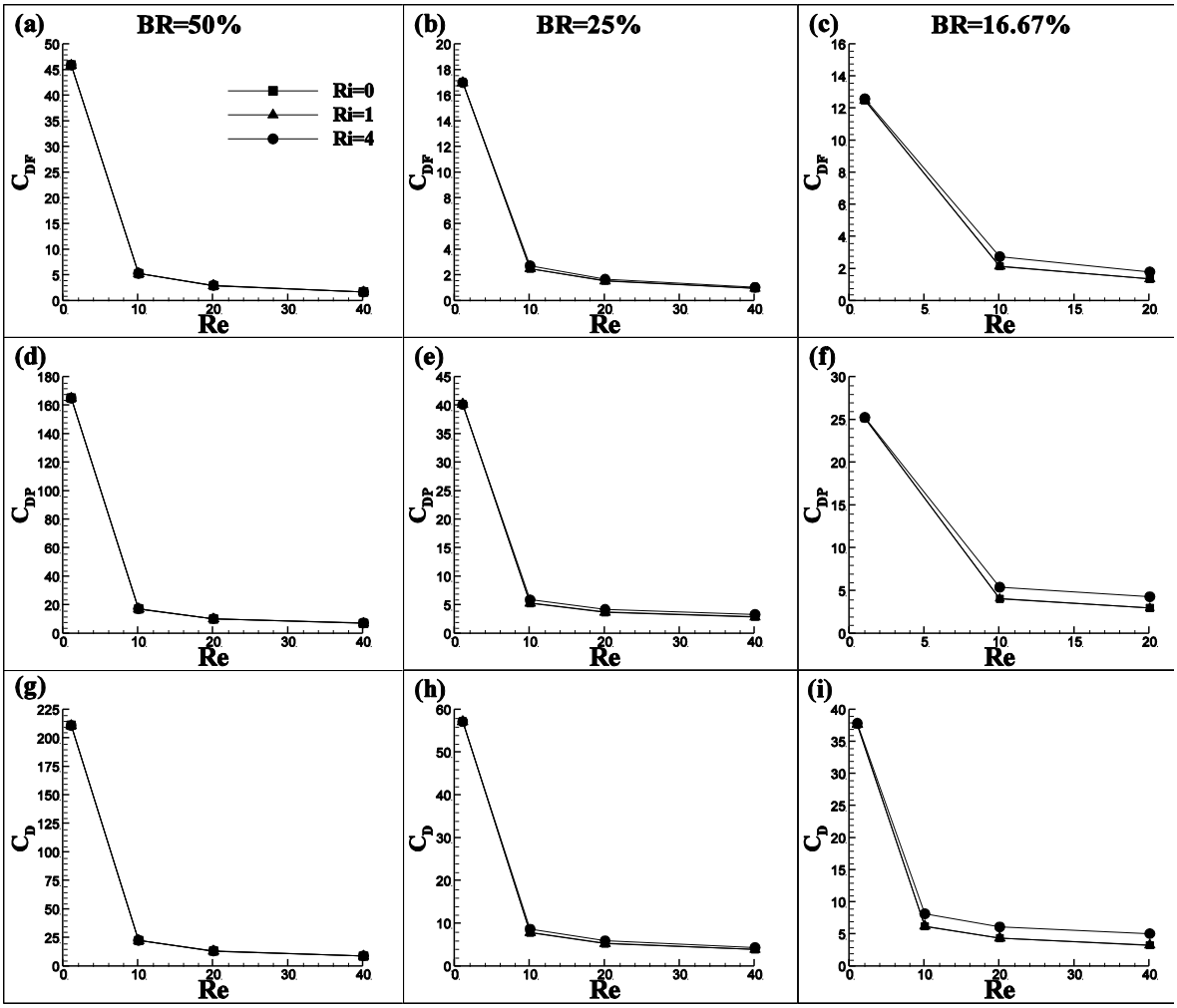


Fig.5: Variation of (a-c) friction drag coefficient,(d-f) pressure drag coefficient and (g-i) total drag coefficient with Reynolds and Richardson numbers and blockage ratio

## 4.4 VARIATION OF LIFT COEFFICIENT WITH Re, Ri AND $\beta$

The variation of the total lift coefficients ($C_L$) with Reynolds numbers is plotted for the ranges of Richardson numbers and blockage ratios in Fig. 6. For higher blockage ratios (e.g. 25% and 50%), the variation of lift coefficient with Re and Ri is found to be the same. For instance, the lift coefficient decreases with Re up to 20 and 10 for $\beta$ =50%, 25% respectively and thereafter it increases at Ri>0. But for low blockage (16.67%), the $C_L$ with Re varies differently at different Ri. For instance, the $C_L$ decreases with Re up to 10 (for Ri=1) and Re up to 20 (for Ri=4) and thereafter it increases with Re. This is because of the fact that cross-buoyancy effects decrease with increasing wall confinements for the range of setting studied. The lift coefficient is found zero for the forced convection case (Ri=0) for all blockage ratios and Reynolds numbers investigated. The total lift coefficient is decreasing with increase in Richardson number for the constant Reynolds number and blockage ratio for Re>1 and $\beta$ =16.67%-50%. However, an opposite trend is observed at Re=1 for $\beta$ =16.67% and 25%. It can also be notable that the lift coefficient is more sensitive to Ri as compared to drag coefficient and Nusselt number. This observation is also supported by our past studies on the cross-buoyancy mixed convection around a confined square cylinder [25, 26].

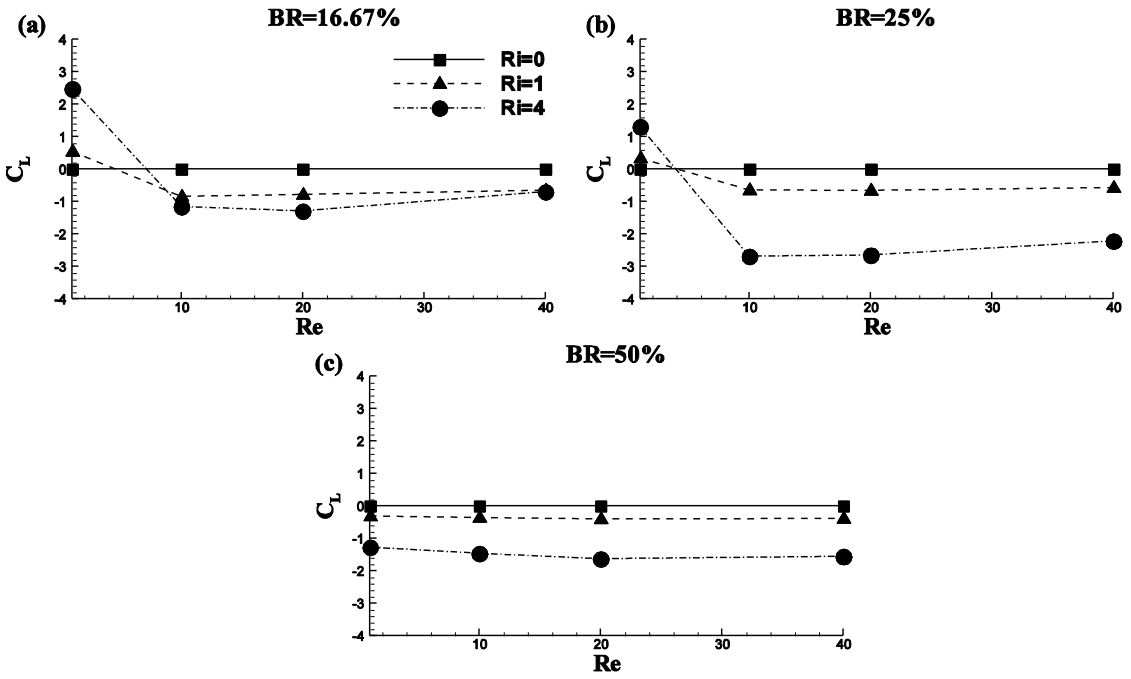


Fig 6: Variation of $C_L$ with Re for different values of Ri and BR

## 4.5 LOCAL AND AVERAGE NUSSELT NUMBERS

The distribution of local Nusselt numbers on the surfaces of a semi-circular cylinder is represented in Fig. 7. The values of local Nusselt numbers on the surfaces of a semi-circular cylinder are increasing with increase in Reynolds number for the constant $\beta$ and Ri, and hence the heat transfer rate will be high at high Reynolds numbers (e.g. Re=40). It also shows heat transfer is high at the front stagnation point of a semi-circular cylinder for the high Reynolds number of 40 and it decreases along the curved surfaces, and the minimum on the rear face (BA). The local Nusselt number increases with increase in blockage ratio for a Reynolds number of 40 (Figs. 7d-7f). At low Reynolds numbers (e.g. Re=1), the highest heat transfer is found to occur at the corners of the flat surface (at A and B) for the blockage ratios of 16.67% and 25%, and this observation is found to be similar to Chandra and Chhabra [18] on the unbounded mixed convection from a semi-circular cylinder. Irrespective of the value of Richardson number, the local Nusselt number is found to be the same for the blockage ratio of 50% at a Reynolds number of unity. The maximum relative enhancement in the value of the local Nusselt number with respect to the forced convection case (Ri=0) is found to be approximately 17% and 44% for Richardson numbers of 1 and 4 respectively for the Reynolds number of 40 and the low blockage ratio of 16.67%. However, the maximum enhancement for the middle blockage ratio of 25% is found to be approximately 8% and 42% for Richardson numbers of 1 and 4 respectively, and the corresponding maximum enhancement for the high blockage ratio of 50% is approximately 5% and 21% respectively for the Reynolds number of 40.

The average Nusselt number is obtained by averaging the local Nusselt number over the curved and flat surfaces of the semi-circular cylinder, and it is illustrated in Figs. 8a-8c for extreme values of Re at different $\beta$ and Ri. It is found that the average Nusselt number increases with increase in Reynolds number for the fixed values of blockage ratio and Richardson number. Likewise, the average Nusselt number increases with increase in Richardson number (similar to ref. [18]) for the value of blockage ratios studied. It can also be notable that at high $\beta$ (=50%) only a slight variation is observed in the values of average Nusselt numbers for various Richardson number and Reynolds number. The average Nusselt number increases with increase in blockage ratio for all Reynolds numbers, except at Re=1 where it decreases with increasing $\beta$. The maximum relative enhancement in the value of the average Nusselt number is found to be approximately 8% as compared to the forced convection case for the Reynolds number of

40, Richardson number of 4 and blockage ratio of 16.67%. Similar to the unbounded semi-circular cylinder [11, 18], the value of the average Nusselt number is found to be higher at the curved portion of the semi-circular cylinder as compared to the flat surface of the semi-circular cylinder. The studies are also conducted for an aiding buoyancy configuration and the result delineating that the aiding buoyancy configuration shows a maximum relative variation of 22% with cross buoyancy configuration for a Reynolds number of 40 and Richardson number of 4.

Furthermore, heat-transfer correlations (Eqs. 4, 5 and 6) are obtained to establish a functional relationship among the Reynolds number, Richardson number, and blockage ratio. For each blockage ratio, 12 data points were used to form the correlations. The following simple correlations can be utilized to calculate the intermediate values of the average Nusselt numbers for the various physical parameters investigated.

For a blockage ratio of 16.67%,

$$\overline{Nu} = 0.88(\mathrm{Re})^{0.39} e^{0.0007Ri} \tag{4}$$

For a blockage ratio of 25%,

$$\overline{Nu} = 0.746(\mathrm{Re})^{0.4546} e^{0.0007Ri} \tag{5}$$

For a blockage ratio of 50%,

$$\overline{Nu} = 1.005\ln(\mathrm{Re})e^{0.00001Ri} + 0.42 \tag{6}$$

Clearly, the average Nusselt number increases with increase in Reynolds number and Richardson number for the blockage ratios of 16.67%, 25% and 50% (Eqs. 4, 5 and 6). It is also found that the Richardson number has only a fewer influence on the average Nusselt number. Equation (4) shows the maximum deviation of about 6.3% and the average deviations of about 1.5%, 1.3% and 0.2% for Ri values of 0, 1 and 4 respectively with the present computed results. Equation (5) shows the corresponding maximum deviation of about 4.8% and the average deviations of about 0.5%, 0.3% and 0.9% for Ri values of 0, 1 and 4 respectively. However, for the blockage ratio of 50%, Eq. (6) shows the maximum deviation of about 7.7% and the average deviations of only about 0.02%, 0.05% and 0.01% for Ri values of 0, 1 and 4 respectively.

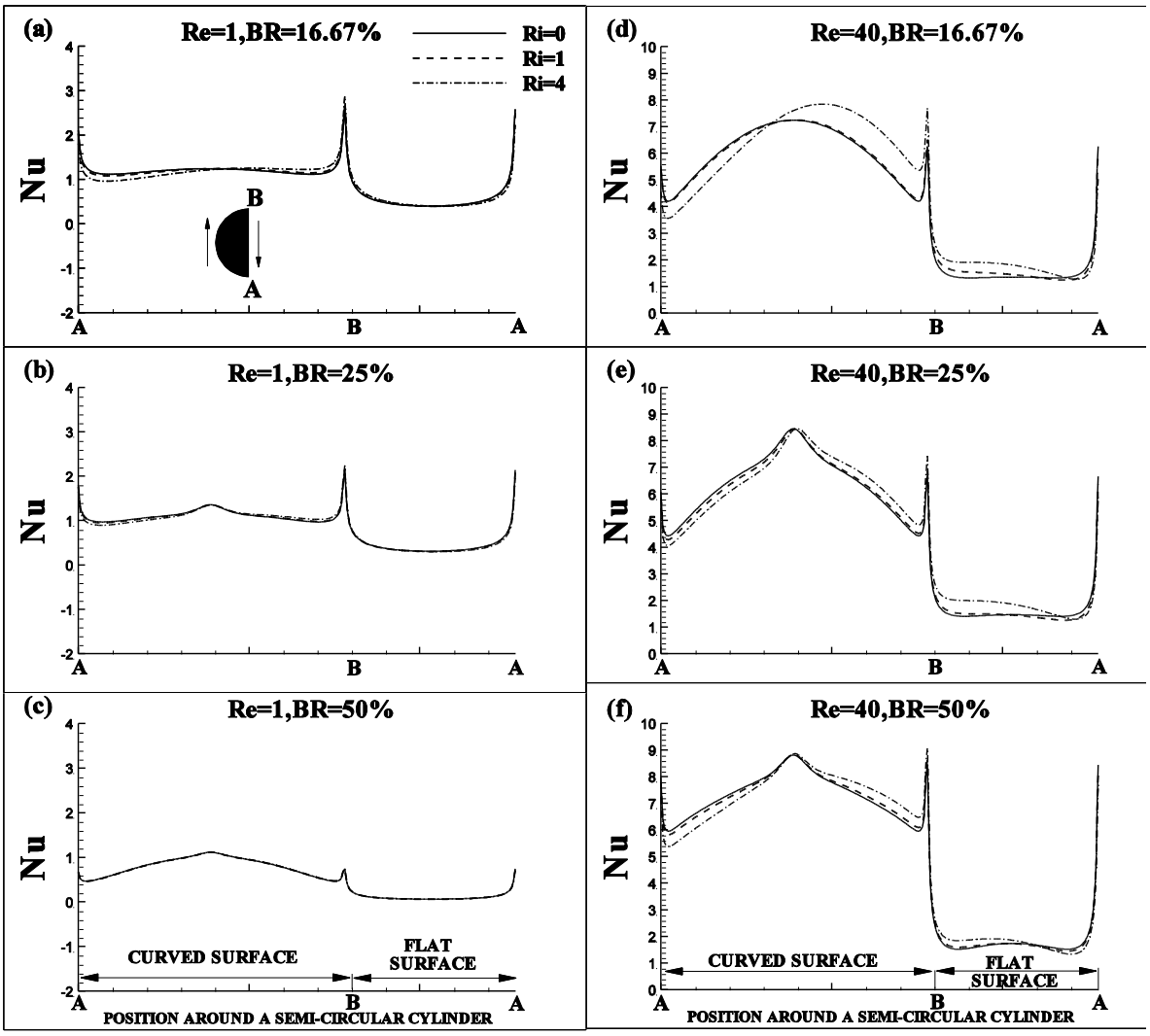


Fig 7: Variation of local Nusselt number around curved and flat surfaces of a semi-circular cylinder for different values of Re, Ri and BR

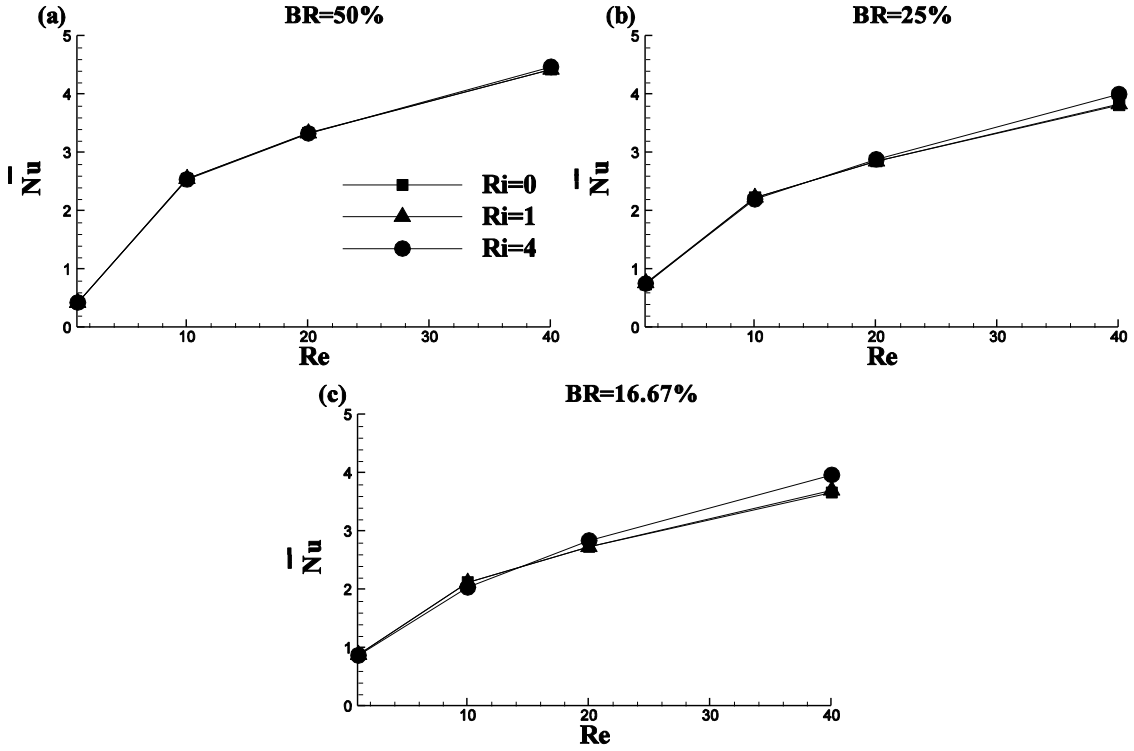


Fig.8: Variation of average Nusselt number with Reynolds and Richardson numbers for different blockage ratios

# Conclusion

In this study, the effects of blockage ratios, Richardson and Reynolds numbers on the cross-buoyancy mixed convection around a confined semi-circular cylinder in a channel are investigated for air. The drag coefficient increases with increase in Richardson number for the constant values of Reynolds number and blockage ratio (16.67% and 25%) and shows a maximum relative enhancement of approximately 55%. However, for the high blockage ratio of 50%, the coefficient of drag is found insensitive to Richardson number. As we move from low blockage ratio (16.67%) to high (50%) for constant Reynolds and Richardson numbers, the drag coefficient increases. The average Nusselt number increases with increase in Richardson number for all the blockage ratios studied. Also, the average Nusselt number increases with increase in blockage ratio for all Reynolds and Richardson numbers except at Re=1. Similar to the unconfined semi-circular cylinder, the average Nusselt number is found to be higher on the curved portion of the semi-circular cylinder where the flow is found to be impinged. Over the ranges of settings covered, the flow is found to be steady except for the Reynolds number of 40, Richardson number of unity and blockage ratio of 16.67%. The maximum relative heat transfer enhancement due to Ri is found to be approximately 8% for Re=40, Ri=4 and for a low wall confinement of 16.67% compared to the forced convection (Ri=0). The aiding buoyancy configuration shows a relative variation of 22% with cross buoyancy configuration for a Reynolds number of 40 and Richardson number of 4. The lift coefficient is found to be more influenced to Ri as compared to drag coefficient and Nusselt number. Lastly, heat-transfer correlations are established for different values of Re, Ri and $\beta$.

# References


[1] M. Kiya, M. Arie, Viscous shear flow past small bluff bodies attached to a plane wall, J. Fluid Mech. 69 (1975) 803-823.

[2] N. Boisaubert, M. Coutanceau, P. Ehrmann, Comparative early development of wake vortices behind a short semi-circular section cylinder in two opposite arrangements, J. Fluid Mech. 327 (1996) 73-99.

[3] N. Boisaubert, M. Coutanceau, A. Texier, Manipulation of the starting semi-circular cylinder near-wake by means of a splitter plate, J. Flow Visual. Image Proc. 4 (1997) 211-221.

[4] N. Boisaubert, A. Texier, Effect of splitter plate on the near-wake development of a semi-circular cylinder, Exp. Ther. Fluid Sci. 16 (1998) 100-111.

[5] M. Coutanceau, C. Migeon, P. Ehrmann, Particulars of the cross and spanwise near-wake development of a short semi-circular section shell, through the transition Re-range (60< Re<600), J. Visual. 3 (2000) 9-26.

[6] M. Kotake, S. Suwa, Flow visualization around a semi-circular cylinder in a uniform shear flow, J. Visual. Society Japan 21 (2001) 95-98.

[7] M. Iguchi, Y. Terauchi, Karman vortex probe for the detection of molten metal surface flow in low velocity range, ISIJ Int. 42 (2002) 939-943.

[8] T. Sophy, H. Sada, R. Bouard, Calcul de l'écoulementautour d'un cylinder semi-circulaire par uneméthode de collocation, C. R. Mecanique 330 (2002) 193–198.

[9] M. Koide, S. Tomida, T. Takahashi, L. Baranayi, M. Shirakashi, Influence of cross-sectional configuration on the synchronization of Karman vortex shedding with the cylinder oscillation, JSME Int. J. Series B 45 (2002) 249-258.

[10] M. Koide, T. Takahashi, M. Shirakashi, Influence of cross-sectional configuration on Karman vortex excitation, J. Comp. Applied Math. 5 (2004) 297-310.

[11] A. Chandra, R.P. Chhabra, Flow over and forced convection heat transfer in Newtonian fluids from a semi-circular cylinder, Int. J. Heat Mass Transfer 54 (2011) 225-241.

[12] A. Gode, A.K. Sahu, R.P. Chhabra, Two-dimensional steady flow over a semi-circular cylinder:`drag coefficient and Nusselt number, Int. J. Adv. Eng. Sci. Appl. Math. 3 (2011) 44-59.

[13] A.S. Bhinder, S. Sarkar, A. Dalal, Flow over and forced convection heat transfer around a semi-circular cylinder at incidence, Int. J. Heat Mass Transfer 55 (2012) 5171–5184.

[14] D. Chatterjee, B. Mondal, P. Halder, Unsteady forced convection heat transfer over a semi-circular cylinder at low Reynolds numbers**,** Numer. Heat Transfer A 63 (2013) 411-429.

[15] A. Chandra, R.P. Chhabra, Influence of power-law index on transition Reynolds number for flow over a semi-circular cylinder, Appl. Math. Model. 35 (2011) 5766-5785.

[16] A. Chandra, R.P. Chhabra, Momentum and heat transfer characteristics of a semi-circular cylinder immersed in power-law fluids in the steady flow regime, Int. J. Heat Mass Transfer 54 (2011) 2734-2750.

[17] G.C. Hocking, J.-M. Vanden-Broeck, The effect of gravity on flow past a semi-circular cylinder with a constant pressure wake, Appl. Math. Model. 32 (2008) 677–687.

[18] A. Chandra, R.P. Chhabra, Mixed convection from a heated semi-circular cylinder to power-law fluids in the steady flow regime, Int. J. Heat Mass Transfer 55 (2012) 214-234.

[19] A. Chandra, R.P. Chhabra, Laminar free convection from a horizontal semi-circular cylinder to power-law fluids, Int. J. Heat Mass Transfer 55 (2012) 2934-2944.

[20] A.K. Tiwari, R.P. Chhabra, Laminar natural convection in power-law liquids from a heated semi-circular cylinder with its flat side oriented downwards, Int. J. Heat Mass Transfer 58 (2013) 553-567.

[21] A. Chandra, R.P. Chhabra, Momentum and heat transfer from a semi-circular cylinder to power-law fluids in the vortex shedding regime, Numer. Heat Transfer A 63 (2013) 411-429.

[22] O. F. Can, N. Celik, Numerical investigation of the effect of flow and heat transfer of a semi-cylindrical obstacle located in a channel, World Academy Sci. Eng. Tech. 77 (2013) 367-371.

[23] S. Singh, G. Biswas, A. Mukhopadhyay, Effect of thermal buoyancy on the flow through a vertical channel with a built-in circular cylinder, Numer. Heat Transfer A 34 (1998) 769–789.

[24] V.S.G. Gandikota, S. Amirroudine, D. Chatterjee, G. Biswas, Effect of aiding/opposing buoyancy on two-dimensional laminar flow and heat transfer across a circular cylinder, Numer. Heat Transfer A 58 (2010) 385–402.

[25] A.K. Dhiman, R.P. Chhabra, V. Eswaran, Steady mixed convection across a confined square cylinder, Int. Comm. Heat Mass Transfer 35 (2008) 47–55.

[26] A.K. Dhiman, N. Sharma, S. Kumar, Wall effect on the cross-buoyancy around a square cylinder in the steady regime, Brazilian J. Chem. Eng. 29 (2012) 253-264.

[27] A.K. Dhiman, N. Sharma, S. Kumar, Buoyancy-aided momentum and heat transfer in a vertical channel with built-in square cylinder, Int. J. Sustainable Energy, 2013, in press.

[28] N. Sharma, A.K. Dhiman, S. Kumar, Non-Newtonian power-law fluid flow around a heated square bluff body in a vertical channel under aiding buoyancy, Numer. Heat Transfer A 64 (2013)777-799.

[29] ANSYS User Manual, Ansys Inc., 2009.

[30] A.T. Srinivas, R.P. Bharti, R.P. Chhabra, Mixed convection heat transfer from a cylinder in power-law fluids: effect of aiding buoyancy, Ind. Eng. Chem. Res. 48 (2009) 9735–9754.

[31] D. Chatterjee, B. Mondal, Effect of thermal buoyancy on vortex shedding behind a square cylinder in cross flow at low Reynolds numbers, Int. J. Heat Mass Transfer 54(2011) 5262-5274.